

1 Analytical Solution of Suspended Sediment Concentration Profile: Relevance of
2 Dispersive Flow Term in Vegetated Channels

3 **Wenxin Huai¹, Liu Yang¹, and Yakun Guo²**

4 ¹ State Key Laboratory of Water Resources and Hydropower Engineering Science, Wuhan
5 University, Wuhan, Hubei 430072, China.

6 ² Faculty of Engineering & Informatics, University of Bradford, BD7 1DP, UK.

7
8 Corresponding author: Wenxin Huai (wxhuai@whu.edu.cn)

9 **Key Points:**

- 10 • A dispersive model is proposed to investigate the sediment transport in the vegetated
11 open channels with parameters fitted with experiments.
- 12 • Analytical solution of the vertical suspended sediment concentration profile is derived for
13 submerged and emergent vegetated open channels.
- 14 • The effects of dispersion on suspended sediment concentration in the vegetated channels
15 is demonstrated by the double-averaging method.
16

17 **Abstract**

18 Simulation of the suspended sediment concentration (SSC) has great significance in
19 predicting the sediment transport rate, vegetation growth and the river ecosystem in the vegetated
20 open channel flows. The present study focuses on investigating the vertical SSC profile in the
21 vegetated open channel flows. To this end, a model of the dispersive flux is proposed in which
22 the dispersive coefficient is expressed as partitioned linear profile above or below the half height
23 of vegetation. The double-averaging method, i.e. time-spatial average, is applied to improve the
24 prediction accuracy of the vertical SSC profile in the vegetated open channel flows. The
25 analytical solution of SSC in both the submerged and the emergent vegetated open channel flows
26 is obtained by solving the vertical double-averaging sediment advection-diffusion equation. The
27 morphological coefficient, a key factor of the dispersive coefficient, is obtained by fitting the
28 existing experimental data. The analytically predicted SSC agrees well with the experimental
29 measurements, indicating that the proposed model can be used to accurately predict the SSC in
30 the vegetated open channel flows. Results show that the dispersive term can be ignored in the
31 region without vegetation, while the dispersive term has significant effect on the vertical SSC
32 profile within the region of vegetation. The present study demonstrates that the dispersive
33 coefficient is closely related to the vegetation density, the vegetation structure and the stem
34 Reynolds number, but has little relation to the flow depth. With a few exceptions, the absolute
35 value of the dispersive coefficient decreases with the increase of the vegetation density and
36 increases with the increase of the stem Reynolds number in the submerged vegetated open
37 channel flows.

38 **Keywords**

39 Suspended sediment concentration; Double-averaging method; Dispersive flow;
40 Vegetated open channel flows;

41

42 **1 Introduction**

43 Aquatic vegetation in the vegetated open channel flows can significantly affect flow
44 velocity and turbulence structure and momentum exchange processes (Huai et al., 2009a; Nepf,
45 2012; Li et al., 2015; Li et al., 2019) as well as the sediment transport (Le Bouteiller & Venditti,
46 2015; Li & Katul, 2019; Yang & Nepf, 2019). Previous studies (Wang et al., 2016; Li et al.,
47 2018) showed that the vertical profile of suspended sediment concentration (referred as SSC
48 hereafter), an important characteristic for waterway ecosystem, is much more complicated in the
49 vegetated open channels than that in channels without vegetation, due to the great variation of
50 the turbulent strength in the vertical direction. Studies of Kim et al. (2018) and Västilä and
51 Järvelä (2018) on the suspended sediment deposition within and around a circular vegetation
52 patch showed that the vegetation enhanced the deposition of sediment in the vegetation region.
53 These studies showed that aquatic vegetation greatly affects the sediment transport rate. The
54 previously dominant methodologies of simulating the suspended sediment transport are based on
55 the time-averaging Navier-Stokes equations or advection-diffusion equations, including turbulent
56 diffusion model (Li et al., 2018; Kundu, 2019), two-phase flow model (Fu et al., 2005) and flume
57 experimental model (Kim et al., 2018; Västilä & Järvelä, 2018). In the vegetated open channels,
58 the spatial heterogeneity of flow field is significantly enhanced by the presence of aquatic
59 vegetation. In order to improve the simulation accuracy in the vegetated open channel flows, the

60 double-averaging methodology is introduced to extend the time averaging flow field to time-
61 spatial averaging field (Nikora et al., 2007a; Wang et al., 2014).

62 The double-averaging method is usually applied to the large eddy simulation (LES),
63 direct numerical simulation (DNS) and physical model to study the spatial heterogeneity in the
64 open channel flow and airflow. To investigate the impact of heterogeneity on edge-flow
65 dynamics, Boudreault et al. (2017) applied double-averaging method to the LES to simulate the
66 forest-edge flows. Their results showed that the forest heterogeneity facilitated flow penetration
67 into the vegetation (i.e. trees and plants). In the roughness region, e.g. rough bed, the
68 heterogeneity is strong. Stoesser and Nikora (2008) and Han et al. (2017) applied the LES with
69 the double-averaging method to evaluate the effect of the roughness on the rough-bed flows. In
70 addition, Coceal et al. (2006, 2007, 2008) used the regular arrays of cubical obstacles as the
71 rough-bed to study the turbulent flow and the dispersive stress in roughness flows with the DNS
72 and the double-averaging method. Laboratory experiment is another methodology to study the
73 flow with spatial heterogeneity. Poggi and Katul (2008a) and Moltchanov et al. (2015) carried
74 out flume experiments to investigate the effect of the spatial heterogeneity on the flow structure
75 in the vegetated open channel flows, while Spiller et al. (2015) conducted flume experiments to
76 examine the role of the heterogeneity in non-uniform steady and unsteady flow over a rough bed.
77 These numerical and experimental studies showed that the double-averaging method can reduce
78 the inconvenience of time-averaging variables in volume resulted from the spatial heterogeneity.
79 In addition, the dispersive flux (or stress), an additional key term in the double-averaging
80 method, is generated due to the deviation of time averaging field from space averaging field
81 (Tanino & Nepf, 2008a).

82 So far the dispersive term in the vegetated open channels has been poorly defined,
83 making it difficult to clearly express the dispersive stress. Florens et al. (2013) conducted
84 laboratory experiments and measured the fluctuation velocity using particle image velocimetry
85 (PIV) to investigate the dispersive stress in the vegetated open channel flows. Poggi et al.
86 (2004a, 2004b) and Poggi and Katul (2008b) conducted flume experiments with the submerged
87 vegetation made of rigid cylindrical rods. They found that the maximum value of the dispersive
88 stress had comparable magnitude (almost 30% of the total stress) with the Reynolds stress
89 (almost 70% of the total stress) within the vegetation region for sparse vegetated flow and was
90 trivial for dense vegetated flow. They also found that the dispersive stress appeared to decrease
91 with the increase of vegetation density. Righetti (2008) conducted experiment with the natural
92 vegetation (*salix pentandra*) and showed that the dispersive stress was large and could not be
93 ignored in natural flexible vegetated flow. These experimental studies revealed that (i) the
94 dispersive stress was significant within the vegetation region, insignificant in the region without
95 vegetation; and (ii) the value of the dispersive stress reached the maximum value at the position
96 close to the half height of vegetation and gradually decreased toward both the channel bottom
97 and the water surface. In addition, the dispersive stress is not only significant in the vegetated
98 flow, but also in the rough-bed flow (Nikora et al., 2007b). The study of Nikora et al. (2007b) for
99 the flow over a rough-bed showed that the double-averaging method could identify the specific
100 flow layers and flow types and the dispersive stress existed in the roughness region of the rough-
101 bed flow.

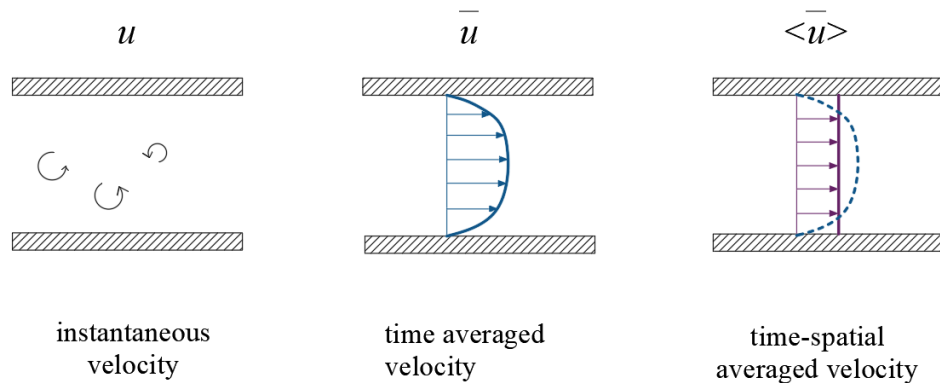
102 Most previous studies only focused on the phenomenon of the dispersive stress. To the
103 authors' best knowledge, so far little knowledge exists about the effect of the dispersive flux on
104 the vertical SSC profile, the application of the dispersive term on the mass transport and the

105 model of the dispersive coefficient. This motivates this study, which focuses on developing a
 106 new dispersive coefficient model and investigating the relationship of dispersive strength with
 107 canopy density and the vertical SSC profile in the steady vegetated open channel flows.
 108 Recently, Tai and Huang (2019) simulated the suspended sediment transport with the stochastic
 109 Lagrangian model. However, their simulated vertical SSC profile was inconsistent with the
 110 experimental observations (see Figure 11 in the literature of Tai and Huang (2019)). Huai et al.
 111 (2019) took dispersion into account and applied the random displacement model, also a
 112 Lagrangian model, to simulate the vertical SSC profile in the vegetated open channel flows.
 113 Though their simulated results were almost consistent with the experimental observations, some
 114 deviation still existed in the region of vegetation for the submerged vegetated open channel flow.
 115 The reason for this deviation in the vegetation region may be due to the hypothesis that the
 116 profile of the dispersive coefficient was the same as the turbulent diffusion coefficient with
 117 different magnitude. This could mean that the distribution of the dispersive coefficient is
 118 different from the turbulent diffusion coefficient in the vegetated open channel flows. Yuuki and
 119 Okabe (2002) used the dispersive coefficient, the averaged longitudinal flow velocity of cross-
 120 section and the averaged SSC of cross-section to model the dispersive flux. As discussed above,
 121 the comparable magnitude of dispersion only exists in the vegetation region and the local SSC
 122 differs from the averaged SSC of cross-section. Therefore, from the point of view of the
 123 physical mechanism, it will be much better to use the local SSC to scale the dispersive flux. In
 124 order to improve the simulation of the vertical SSC profile, in this study, the double-averaging
 125 method is thus applied to investigate the sediment transport in the vegetated open channel flows
 126 by assuming that the dispersive term only exists in the vegetation region. In order to reduce the
 127 deviation caused by the application of the averaged SSC of cross-section, a new approximation
 128 approach is then proposed in this study to express the dispersive flux of suspended sediment,
 129 where the dispersive flux is proportional to the local SSC in the vegetated open channel flows.
 130 The analytical solution of the vertical SSC profile is obtained by solving the double-averaging
 131 advection-diffusion equations, which are influenced by vegetation density, vegetation structure,
 132 flow characteristics and the spatial arrangement of vegetation.

133

134 2 Theory

135 2.1 Double-averaging Method



136

137

Figure 1. The schematic diagram of time-spatial averaging method for platform flow.

138 Though the double-averaging method can be found in previous studies (e.g. Nikora et al.,
 139 2007a, b), we present a brief description for convenience and completeness. To this end, the flow
 140 between the platforms, as shown in Figure 1, is taken as an example to demonstrate the concept
 141 of the double-averaging method. The instantaneous longitudinal flow velocity (denoted as u) can
 142 be decomposed as $u = \bar{u} + u'$ based on the Reynold's decomposition approach, while the time-
 143 averaging velocity can be further decomposed as $\bar{u} = \langle \bar{u} \rangle + u''$. In these decompositions, the
 144 overbar denotes the time averaged variables, the single prime represents the fluctuation velocity,
 145 i.e. the deviation of instantaneous variables from the time-averaging variables, the double primes
 146 denotes the time averaged deviations from spatial averaged variables and the symbol $\langle \rangle$
 147 represents the spatially averaged variables. Instantaneous velocity, therefore, can be expressed as
 148 $u = \langle \bar{u} \rangle + u'' + u'$ in the time-spatial averaging flow field. This means that the double-averaging
 149 method includes two main steps: (1) firstly applying time averaging to the equations for
 150 instantaneous variables; (2) secondly applying the spatial averaging to the equations which have
 151 already been averaged in the time domain.

152 Though the double-averaging method has been widely applied to investigate the flow
 153 field in rough open channel and river flow, the method has been hardly ever applied to estimate
 154 the vertical SSC profile in the vegetated open channel flows. In this paper, the authors will
 155 propose a new model for describing the dispersion in sediment-laden flow with vegetation and
 156 apply the double-averaging method to calculate the vertical SSC profile. The instantaneous
 157 advection-diffusion equation of sediment is written as following based on the mass conservation:

$$158 \quad \frac{\partial c}{\partial t} + \frac{\partial(u_j c)}{\partial x_j} - \frac{\partial}{\partial x_j} \left(K_m \frac{\partial c}{\partial x_j} \right) + S = 0 \quad (1)$$

159 where t represents time, c is the instantaneous SSC, x_j is the j th direction ($x_1 = x$ represents the
 160 longitudinal direction; $x_2 = y$ represents the transverse direction; $x_3 = z$ represents the vertical
 161 direction), u_j ($j=1, 2$ and 3) is the instantaneous flow velocity component in the directions of x , y
 162 and z , respectively; K_m represents the molecular diffusion coefficient and S represents the source
 163 or sink of sediment. The first term in Equation (1) is the variation of SSC with time, the second
 164 term represents the transport of sediment advection flux in the x_j direction and the third term is
 165 the transport of sediment molecular diffusion flux.

166 Applying the double-averaging approach by inserting the decomposed instantaneous
 167 variables of c , u_j and S as $\varphi = \bar{\varphi} + \varphi'$ (where φ represents the variables) into Equation (1)
 168 yields:

$$169 \quad \frac{\partial}{\partial t} (\bar{c} + c') + \frac{\partial}{\partial x_j} [(\bar{u}_j + u_j')(\bar{c} + c')] - \frac{\partial}{\partial x_j} \left(K_m \frac{\partial (\bar{c} + c')}{\partial x_j} \right) + \bar{S} + S' = 0 \quad (2)$$

170 Applying time-averaging to Equation (2) yields:

$$171 \quad \frac{\partial}{\partial t} (\overline{\bar{c} + c'}) + \frac{\partial}{\partial x_j} \left[\overline{(\bar{u}_j + u_j')(\bar{c} + c')} \right] - \frac{\partial}{\partial x_j} \left(\overline{K_m \frac{\partial (\bar{c} + c')}{\partial x_j}} \right) + \bar{S} + \bar{S}' = 0 \quad (3)$$

172 According to the rules: $\overline{f + \varphi} = \overline{f} + \overline{\varphi}$, $\overline{\sigma f} = \sigma \overline{f}$ and $\overline{f'} = 0$ (where f represents a
 173 variable and σ is a constant), Equation (3) can be simplified as (Tanino & Nepf, 2008a; Termini,
 174 2019):

$$175 \quad \frac{\partial \overline{c}}{\partial t} + \frac{\partial}{\partial x_j} (\overline{u_j c} + \overline{u_j' c'}) - \frac{\partial}{\partial x_j} \left(K_m \frac{\partial \overline{c}}{\partial x_j} \right) + \overline{S} = 0 \quad (4)$$

176 Using the decomposition of \overline{c} , $\overline{u_j}$ and \overline{S} as $\overline{\varphi} = \langle \overline{\varphi} \rangle + \varphi''$, applying the spatial-averaging
 177 method and according to the rules: $\langle \varphi'' \rangle = 0$ and $\langle \langle \overline{\varphi} \rangle \rangle = \langle \overline{\varphi} \rangle$, Equation (4) can be expressed as:

$$178 \quad \frac{\partial \langle \overline{c} \rangle}{\partial t} + \frac{\partial (\langle \overline{u_j} \rangle \langle \overline{c} \rangle)}{\partial x_j} + \frac{\partial (\langle \overline{u_j' c'} \rangle + \langle u_j'' c'' \rangle)}{\partial x_j} - \frac{\partial}{\partial x_j} \left(K_m \frac{\partial \langle \overline{c} \rangle}{\partial x_j} \right) + \langle \overline{S} \rangle = 0 \quad (5)$$

179 Equation (5) is the double-averaging advection-diffusion equation. The first term of the
 180 Equation (5) expresses the variation of the double-averaging SSC with time. The second term is
 181 the transport of advection flux resulted from the averaged flow velocity. The third term is the
 182 transport of diffusive flux related to the turbulent fluctuations u_j' and the fourth term is the
 183 transport of the dispersive flux associated with the spatial heterogeneity of time-averaging
 184 velocity field. The molecular diffusion term is ignored as it is much smaller than the turbulent
 185 diffusion and the dispersive flux. Assuming that no sediment is added into the river, therefore,
 186 the sediment source/sink term $\langle \overline{S} \rangle$ can be written as $-\partial(\omega \langle \overline{c} \rangle) / \partial x_3$ (i.e. the transport of
 187 sediment settling flux) in sandy flow, where ω is the settling velocity of sediment particles.

188 Furthermore, in the steady uniform open channel flow, one has $\frac{\partial \langle \overline{c} \rangle}{\partial t} = 0$, $\partial(\langle \overline{u_j} \rangle \langle \overline{c} \rangle) / \partial x_j = 0$
 189 for $j=1, 2$ and 3 , $\partial(\langle \overline{u_j' c'} \rangle) / \partial x_j = 0$ and $\partial(\langle u_j'' c'' \rangle) / \partial x_j = 0$ for $j=1, 2$ (i.e. in both the
 190 longitudinal and the transverse directions). Equation (5) can then be simplified as:

$$191 \quad \frac{\partial}{\partial x_3} (\langle \overline{u_3' c'} \rangle + \langle u_3'' c'' \rangle) - \frac{\partial (\omega \langle \overline{c} \rangle)}{\partial x_3} = 0 \quad (6)$$

192 The additional dispersive flux term needs to be appropriately determined in order to
 193 accurately simulate the vertical SSC profile in the steady equilibrium vegetated open channel
 194 sediment-laden flow.

195

196 2.2 The Dispersive Flux

197 The turbulent diffusion flux in Equation (6) is determined by the Fickian transport theory
 198 (van Rijn, 1984; Yang & Choi, 2010; Termini, 2019):

$$199 \quad \langle \overline{u_3' c'} \rangle = -K_z \frac{\partial \langle \overline{c} \rangle}{\partial x_3} = -K_z \frac{\partial C}{\partial z} \quad (7)$$

200 where K_z represents the vertical turbulent diffusion coefficient. In Equation (7), for
 201 simplification, $\langle \bar{c} \rangle$ is replaced by C to represent the time-spatial averaged SSC.

202 In flow without vegetation, the dispersive flux is usually ignored as it is much smaller
 203 than the turbulent flux. However, in the vegetated open channel flow, the dispersive flux cannot
 204 be ignored as the spatial heterogeneity is significantly strengthened by the presence of
 205 vegetation. This indicates that the dispersive flux has great effect on the vertical SSC profile in
 206 the vegetated open channel flow. In this study, we assume that the dispersive flux can be
 207 expressed as following:

$$208 \quad \langle u_3 "c" \rangle = -K_D UC \quad (8)$$

209 where K_D is the dispersive coefficient, U is the longitudinal averaged velocity of cross-section
 210 and is used to scale the magnitude of the vertical averaged velocity that is difficult to obtain.
 211 Substituting Equations (7) and (8) into Equation (6) yields:

$$212 \quad \frac{\partial}{\partial z} \left(-K_z \frac{\partial C}{\partial z} - K_D UC \right) - \frac{\partial(\omega C)}{\partial z} = 0 \quad (9)$$

213 The sediment advection-diffusion equation of fully developed steady flow can then be simplified
 214 as following:

$$215 \quad \omega C + K_z \frac{dC}{dz} + K_D UC = A \quad (10)$$

216 where A is an integral constant. Equation (10) shows that the first term (the downward sediment
 217 settling flux) has to balance with the second and third terms (the upward diffusion and the
 218 dispersive fluxes). As no sediment is added into or jumps out of river at the water surface, the
 219 integral constant A is equal to zero. The Equation (10) then becomes:

$$220 \quad \omega C + K_z \frac{dC}{dz} + K_D UC = 0 \quad (11)$$

221 The vertical SSC profile in the steady vegetated open channel flows can then be obtained by
 222 solving Equation (11).

223 In this study, the dispersive coefficient K_D that is related to the spatial heterogeneity in
 224 the vegetated open channel flow is defined as a function of the vertical coordinate z . In order to
 225 simplify the dispersive model, we assume that the dispersive coefficient is equal to the product of
 226 a scale factor K_f multiplying the morphological coefficient k_m :

$$227 \quad K_D = K_f k_m \quad (12)$$

228 where the morphological coefficient k_m is a parameter reflecting the impact of flow field and
 229 vegetation (including the vegetation density, structure and arrangement) on dispersion; the scale
 230 factor $K_f=0.001$ is used to eliminate the influence induced by the application of the longitudinal
 231 sediment flux UC rather than the vertical sediment flux $u_3 C$ as well as to express the magnitude
 232 of the dispersive coefficient. Simulation shows that it is appropriate for the conditions
 233 investigated in this proposed model. According to the variation rules of the dispersive
 234 coefficient, k_m is equal to zero in the flow without vegetation, where the magnitude of the
 235 dispersion term is much smaller than the diffusion and advection terms.

236 The effect of dispersion is significant due to strong heterogeneity generated by the
 237 presence of vegetation. As discussed above, extensive experimental studies have been conducted
 238 to investigate the profile of the dispersive stress in the vegetated open channel flow. These
 239 studies (Poggi et al., 2004a; Rightetti, 2008; Stoesser & Nikora, 2008) showed that the variation
 240 of the dispersive stress was complicated but followed the similar law. They (Poggi et al., 2004a;
 241 Rightetti, 2008; Stoesser & Nikora, 2008) found that the dispersive stress increased from the zero
 242 at the channel bottom and reached the maximum value at almost the half height of vegetation
 243 and then decreased and approached zero at the top of vegetation. As such, the morphological
 244 coefficient can be parameterized as following:

$$245 \quad k_m = \begin{cases} 0 & z \geq h & (a) \\ -\frac{2\theta}{h}z + 2\theta & \frac{h}{2} \leq z < h & (b) \\ \frac{2\theta}{h}z & z < \frac{h}{2} & (c) \end{cases} \quad (13)$$

246 where h is the height of vegetation and the parameter θ is the value of the morphological
 247 coefficient at the half height of vegetation, where coefficient k_m reaches the maximum value.
 248 Equations (12) and (13) show that the dispersive coefficient is known when the value of θ is
 249 determined. The maximum value of the morphological coefficient can be obtained by fitting the
 250 available experimental data of SSC for various vegetation conditions.

251 3 Method

252 In order to investigate the effect of the dispersive flux on the vertical SSC profile in the
 253 vegetated open channel flow, the turbulent diffusion flux and the sediment settling flux need to
 254 be determined. Nepf et al. (2004) conducted experiments to investigate the characteristic of the
 255 turbulent diffusion using the rigid straight rods as vegetation. The results showed that the
 256 turbulent diffusion coefficient approximated to the linear profile within the region of vegetation
 257 in the submerged vegetated open channel flow. The turbulent diffusion coefficient reached the
 258 maximum value at the top of vegetation and decreased linearly toward the water surface. Several
 259 formulas were proposed to simulate the turbulent diffusion coefficient in channels with the
 260 submerged vegetation. However, the turbulent diffusion coefficient remains almost a constant in
 261 the emergent vegetated open channel flow (Nepf, 1999). The settling velocity of sediments is
 262 another important parameter and can be estimated using the formula proposed by Zhang and Xie
 263 (1989) (see also Tan et al., 2018), which is applicable for both the laminar and the turbulent
 264 flow:

$$265 \quad \omega = \sqrt{\left(13.95 \frac{\nu}{d}\right)^2 + 1.09 \frac{\gamma_s - \gamma_f}{\gamma_f} gd} - 13.95 \frac{\nu}{d} \quad (14)$$

266 where ν represents the kinematic viscosity of water, g is the acceleration of gravity, γ_s and γ_f
 267 represent the bulk density of sediment and water, respectively, d is the representative size of
 268 sediment particles and the median size of sediments is used in this study.

269 The analytical solution of the vertical SSC profile can be obtained by solving the
 270 Equation (11) with the turbulent diffusion coefficient, the sediment settling velocity, as well as
 271 the dispersive coefficient determined in different vegetated open channel flows. The following
 272 sections introduce the methods for channels with the emergent and the submerged vegetation,
 273 respectively.

274

275 3.1 Channels with the Emergent Vegetation

276 Previous studies showed that majority of the flow momentum is absorbed by the
 277 vegetation elements induced drag instead of the resistance generated by channel bed in the
 278 vegetated open channel flows (Wilson, 2007; Tanino & Nepf, 2008b). The vertical turbulent
 279 diffusion coefficient $K_z(z)$ is homogenized due to the presence of the emergent aquatic vegetation
 280 (Nepf, 1999, 2004) and can be expressed as the following in dense vegetation flow ($a_v h > 0.1$)
 281 with the emergent cylindrical stems of uniform diameter:

$$282 \quad K_z = \alpha^3 \sqrt[3]{C_D a_v D U D} \quad (15)$$

283 where D is the diameter of vegetation stem, C_D is the drag coefficient of vegetation, a_v is the
 284 frontal area density of vegetation (expressed as $a_v = nD$, n is the number of vegetation per unit
 285 area of channel bed) and α is a proportional factor, which is taken as 0.2 for the vertical
 286 turbulent diffusion coefficient and as 0.8 for the lateral turbulent diffusion coefficient in the
 287 emergent vegetated open channel flow (Nepf, 2004). In addition, α should slightly increase for
 288 the condition of dense vegetation. The value of C_D significantly depends on the density of
 289 vegetation and flow Reynolds number (Sonnenwald et al., 2019). In present study, according to
 290 the balance of vegetation drag with the streamwise component of gravity, the drag coefficient is
 291 evaluated as $C_D = 2gs / (a_v U^2)$ (where s is the slope of channel bed) for experimental conditions
 292 of different vegetation densities (Huai et al., 2009b).

293 As the dispersive coefficient is different in the regions of $z > h/2$ and $z < h/2$, the analytical
 294 solution of Equation (11) should be solved respectively at different layers with $z = h/2$ as the
 295 critical height. Integrating Equation (11) using the turbulent diffusion coefficient determined by
 296 Equation (15) and the dispersive coefficient determined by Equations (12) and (13) yields the
 297 profiles of the vertical SSC in the emergent vegetated open channel flow:

$$298 \quad C = C_a \exp\left(\frac{\theta K_f U}{h K_z} (z^2 - z_a^2) - \frac{2\theta K_f U + \omega}{K_z} (z - z_a)\right) \quad \text{for } z \geq \frac{h}{2} \quad (16a)$$

$$299 \quad C = C_a \exp\left(-\frac{\theta K_f U}{h K_z} \left(z^2 - \frac{h^2}{4}\right) - \frac{\omega}{K_z} \left(z - \frac{h}{2}\right)\right) \quad \text{for } z < \frac{h}{2} \quad (16b)$$

300 where z_a and C_a are the referenced height and the corresponding referenced SSC, respectively. In
 301 this study, z_a is taken as the half height of the flow depth, namely $z_a = H/2$ (H is the flow depth)
 302 and $H = h$ in the emergent vegetated flow.

303 Experiments conducted by Lu (2008) and Ikeda et al. (1991) are used to fit the dispersive
 304 coefficient and to validate the analytical model. The experimental parameters are summarized in
 305 Table 1. In their experiments, SSC was measured in the emergent vegetated (rigid cylindrical

306 rods) flow for various vegetation densities. To calculate the vertical SSC profile, the turbulent
 307 diffusion coefficient K_z is calculated by using Equation (15) for experiments of Lu (2008). For
 308 comparing with the experiment of Ikeda et al. (1991) whose experimental vegetation density is
 309 beyond the applicable scope of Equation (15), K_z is, therefore, obtained as $K_z = 0.09u_*h$
 310 (where u_* is the friction velocity of flow), as suggested by Ikeda et al. (1991).

311

312 **Table 1.** Experimental parameters of Lu (2008) and Ikeda et al. (1991) in the emergent
 313 vegetated open channel flows.

Sources	Run number	$h(H)$ (m)	D (m)	s (10^{-3})	U (m/s)	u_* (m/s)	d (mm)	a_v (m^{-1})	C_D /
Lu	D12-1	0.12	0.006	13.6	0.3343	0.1265	0.217	2.4	0.99
	D12-2	0.12	0.006	13.6	0.2918	0.1265	0.217	3.0	1.04
	D12-3	0.12	0.006	13.6	0.1690	0.1265	0.217	6.0	1.56
	D15-1	0.15	0.006	13.6	0.3321	0.1414	0.217	2.4	1.01
	D15-2	0.15	0.006	13.6	0.2932	0.1414	0.217	3.0	1.03
	D15-3	0.15	0.006	13.6	0.1700	0.1414	0.217	6.0	1.54
	D18-1	0.18	0.006	13.6	0.3436	0.1549	0.217	2.4	0.94
	D18-2	0.18	0.006	13.6	0.2947	0.1549	0.217	3.0	1.02
	D18-3	0.18	0.006	13.6	0.1692	0.1549	0.217	6.0	1.55
Ikeda	Run 9	0.05	0.005	6.67	0.2858	0.0572	0.145	1.0	1.60

314

3.2 Channels with the Submerged Vegetation

315 Flow structure, the turbulent diffusion and the dispersion in the submerged vegetated
 316 flow are much complicated than that in the emergent vegetated flow (Huai et al., 2009b; Nepf,
 317 2012). As the expression of the dispersive and diffusion coefficients changes with water depth,
 318 Equation (11) needs to be solved at three layers to obtain the solution of SSC.

319

320 **Table 2.** Flow and sediment characteristics of experiments of Lu (2008) and Yuuki and Okabe
 321 (2002) in the submerged vegetated flow (k is the von Karman's constant).

Sources	Run number	H (cm)	h (cm)	D (cm)	d (mm)	s (10^{-3})	u_* (cm/s)	U (cm/s)	k /	a_v (m^{-1})
Lu	C12	12	6.0	0.6	0.217	4.65	4.76	27.86	0.25	3
	C15	15	6.0	0.6	0.217	3.50	4.77	29.34	0.27	3
	C18	18	6.0	0.6	0.217	2.69	5.20	32.12	0.28	3
Yuuki and Okabe	Y1	6	3.5	0.2	0.100	1.00	2.13	22.70	0.20	2.08
	Y2	6	3.5	0.2	0.100	1.50	2.60	28.10	0.20	2.08
	Y3	6	3.5	0.2	0.100	2.00	3.01	31.90	0.20	2.08

322

323 Lu (2008) and Yuuki and Okabe (2002) conducted experiments to study the interaction of
 324 the suspended sediment load and vegetation in the submerged vegetated flow. These experiments
 325 are used for comparing and validating the present analytical model. Table 2 lists the parameters

326 and measurements of these two experiments. As the construction of experimental vegetation in
 327 these two experiments differs greatly from each other, the equations of the turbulent diffusion
 328 coefficient are also different, as demonstrated below.

329 Figure 2 is the sketch of the vertical turbulent diffusion coefficient and the morphological
 330 coefficient of the experiments of Lu (2008), in which the vegetation was modeled by rigid
 331 straight rods. Based on the study of Nepf (2012), the maximum value of the turbulent diffusion
 332 coefficient appears at the top of vegetation for flow with dense vegetation ($a_v h > 0.1$) and can be
 333 expressed as:

$$334 \quad K_z(z=h) = 0.032\Delta u h \quad (17)$$

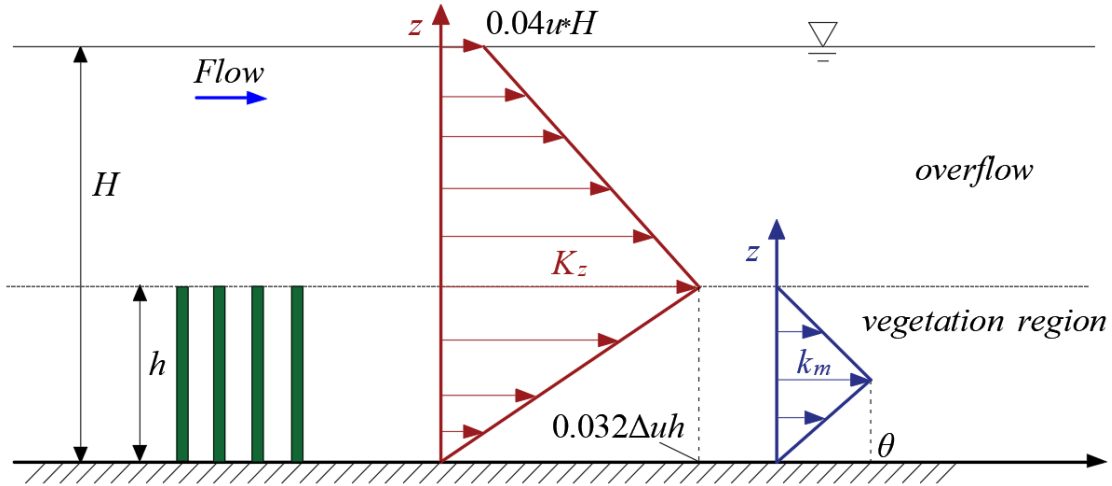
335 where Δu represents the velocity difference between the wake region of vegetation and
 336 overflow, which is approximately equal to $0.8u_H - u_w$ (where u_H is the flow velocity at the water
 337 surface and can be expressed as the logarithmical profile (Huai et al., 2019) and
 338 $u_w = \sqrt{2gs / (C_D a_v)}$ is the averaged velocity in the wake region of vegetation and can be obtained
 339 according to the balance of gravity and drag (Huai et al., 2009b)). The diffusion coefficient is
 340 usually zero at the channel bed. In addition, in order to avoid the obvious mistake that the SSC is
 341 zero at the water surface caused by the approximation of $K_z(z=H)=0$, e.g. the solution of the
 342 classical Rouse equation (Rouse, 1937), the turbulent diffusion coefficient at the water surface of
 343 flow cannot be zero. The study of Elder (1959) showed that the depth-averaging turbulent
 344 diffusion coefficient is equal to $ku_*H/6$. In this study, the von Karman's constant (see Table 2) is
 345 smaller than 0.4, which is the value in clear water flow. For three conditions of Lu (2008), the
 346 mean value of the von Karman's constant k approximates to 0.26. Therefore, the expression of K_z
 347 is approximated as $K_z(z=H) \approx 0.04u_*H$ at the water surface. The results show that the SSC
 348 modeled by this expression is consistent with the experimental observations near the water
 349 surface. After obtaining the values of K_z at three locations, namely the water surface, the top of
 350 vegetation and the channel bed, assuming a linear transition within the region of vegetation and
 351 overflow yields the expression of the vertical turbulent diffusion coefficient:

$$352 \quad K_z = \begin{cases} k_2 z + b_2 & z \geq h \\ k_1 z + b_1 & z < h \end{cases} \quad (18)$$

353 where the parameters k_1 , k_2 , b_1 and b_2 differ in different experimental conditions. For
 354 experiments of Lu (2008), the parameters are calculated as $k_1 = 0.032\Delta u$, $b_1 = 0$,
 355 $k_2 = (0.04u_*H - 0.032\Delta u h) / (H - h)$ and $b_2 = 0.032\Delta u h - k_2 h$. The dispersive coefficient in the
 356 vegetation region is simulated by using Equation (13) and is ignored in the overflow where the
 357 dispersive term is much smaller than the turbulent diffusion term.

358

359

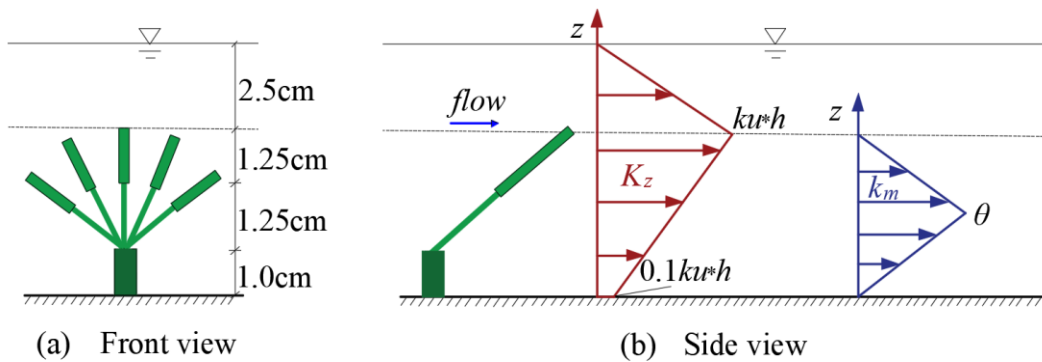


360

361 **Figure 2.** Sketch of the submerged vegetation and the profile of K_z and k_m in the experiment of
 362 Lu (2008).

363

364 Yuuki and Okabe (2002) carried out experiments in which the vegetation was composed
 365 of stagger-arrangement three-layer cylinders with averaged diameter $D=2\text{mm}$, as shown in
 366 Figure 3. The five branches significantly affect the value of the turbulent diffusion and the
 367 dispersive coefficient. Therefore, Equation (17) is not applicable for this experimental condition
 368 as it was established based on the experiments with the vegetation of straight rigid rods.
 369 However, the turbulent diffusion coefficient can still be divided into two layers according to the
 370 height of vegetation and is assumed to be linear profile in each layer (see Figure 3). According to
 371 the study of Yang and Choi (2010), the diffusion coefficient at the top of vegetation is
 372 $K_z(z=h) = ku_*h$, and $K_z(z=0) = 0.1ku_*h$ is used at the bottom of channel where the turbulent
 373 diffusion coefficient is not zero according to the experimental observation in Yuuki and Okabe
 374 (2002). The four parameters are then calculated as $k_2 = \frac{ku_*h}{h-H}$, $b_2 = -\frac{ku_*hH}{h-H}$, $k_1 = 0.8ku_*$ and
 375 $b_1 = 0.1ku_*h$, respectively. The referenced level $z_a=H/2$ is also used for open channel flows with
 376 the submerged vegetation.



377

378 **Figure 3.** The sketch of the vegetation structure, K_z and k_m in the experiment of Yuuki and
 379 Okabe (2002). (a) The front view of the vegetation; (b) The side view of the vegetation, profile
 380 of the turbulent diffusion coefficient and the morphological coefficient.

381

382 The analytical solution of Equation (11) associated with various $K_z(z)$ and k_m can then be
 383 obtained in three layers with some differences for these two experiments of different conditions,
 384 as described below.

385 For experiments of Lu (2008), the referenced height is in the overflow region, i.e. $z_a \geq h$.
 386 In the overflow region ($z \geq h$), the effect of the vegetation induced dispersion is assumed to be
 387 small and can be ignored. Substituting Equations (18) and (13a) into (11), solving the ordinary
 388 differential equation obtains the SSC in the overflow region in the uniform submerged vegetated
 389 flow:

$$390 \quad C(z) = C(z_a) \left(\frac{k_2 z + b_2}{k_2 z_a + b_2} \right)^{\frac{\omega}{k_2}} \quad (19)$$

391 In the upper vegetation region, i.e. $h/2 \leq z < h$, the analytical solution of Equation (11)
 392 with consideration of the dispersion term is:

$$393 \quad C(z) = C(h) \exp\left(\frac{r_1}{k_1}(z-h)\right) \left(\frac{k_1 z + b_1}{k_1 h + b_1}\right)^{\frac{\lambda_1 k_1 - r_1 b_1}{k_1^2}} \quad (20)$$

394 where $r_1 = 2\theta K_f U / h$, $\lambda_1 = -2\theta K_f U - \omega$ and $C(h)$ denotes the SSC at the top of vegetation and
 395 can be calculated by Equation (19) as following:

$$396 \quad C(h) = C_a \left(\frac{k_2 h + b_2}{k_2 z_a + b_2} \right)^{\frac{\omega}{k_2}} \quad (21)$$

397 The analytical solution of SSC in the lower vegetation region (i.e. $z < h/2$) is:

$$398 \quad C(z) = C\left(\frac{h}{2}\right) \exp\left(\frac{r_2}{k_1}\left(z - \frac{h}{2}\right)\right) \left(\frac{k_1 z + b_1}{k_1 \frac{h}{2} + b_1}\right)^{\frac{\lambda_2 k_1 - r_2 b_1}{k_1^2}} \quad (22)$$

399 where $r_2 = -2\theta K_f U / h$, $\lambda_2 = -\omega$ and $C(h/2)$ represents the SSC at the half height of vegetation
 400 and can be calculated by Equation (20).

401 In the experiments of Yuuki and Okabe (2002), the referenced height is within the
 402 vegetation region, i.e. $h/2 < z_a = H/2 < h$. Therefore, the analytical solution of the profile of SSC
 403 differs from above. In the upper vegetation region, i.e. $h/2 \leq z \leq h$, the analytical solution of
 404 Equation (11) with consideration of the dispersion term is:

$$C(z) = C(z_a) \exp\left(\frac{r_1}{k_1}(z - z_a)\right) \left(\frac{k_1 z + b_1}{k_1 z_a + b_1}\right)^{\frac{\lambda_1 k_1 - r_1 b_1}{k_1^2}} \quad (23)$$

In the overflow region ($z > h$), the effect of vegetation induced dispersion is assumed to be small and can be ignored. Substituting Equations (18) and (13a) into (11) and solving the (11) yields SSC:

$$C(z) = C(h) \left(\frac{k_2 z + b_2}{k_2 h + b_2}\right)^{-\frac{\omega}{k_2}} \quad (24)$$

where $C(h)$ can be calculated by the Equation (23).

The analytical solution of SSC in the lower vegetation region (i.e. $z < h/2$) is:

$$C(z) = C\left(\frac{h}{2}\right) \exp\left(\frac{r_2}{k_1}\left(z - \frac{h}{2}\right)\right) \left(\frac{k_1 z + b_1}{k_1 \frac{h}{2} + b_1}\right)^{\frac{\lambda_2 k_1 - r_2 b_1}{k_1^2}} \quad (25)$$

where $C(h/2)$ represents the SSC at the half height of vegetation and can be calculated by Equation (23).

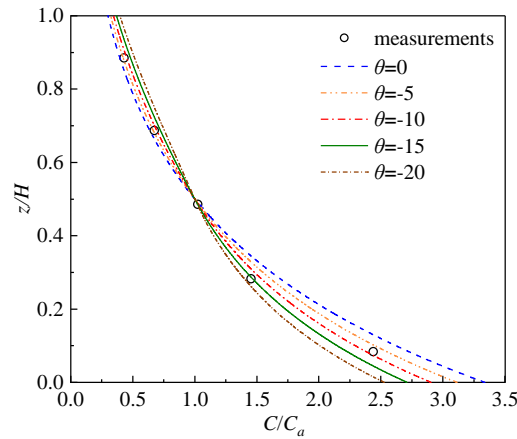
4 Results

4.1 Emergent Vegetation

Figures 4 and 5 show the comparison of the predicted and measured vertical profiles of SSC for experiments of Ikeda et al. (1991) and Lu (2008), respectively. It is seen that the analytical solution ignoring the dispersive term, i.e. $\theta=0$ (blue dashed lines in Figures 4 and 5), greatly under-predicts SSC above the half height of flow depth and significantly over-predicts SSC within half height of flow depth. This indicates that the effect of the dispersive flux on the vertical SSC distribution in the vegetated open channel flows is significant and cannot be ignored in calculating the vertical SSC profile. It is seen from Figures 4 and 5 that the dispersive coefficient is usually negative, which means that the direction of the dispersive flux is opposite to the settling flux. According to the mass conservation, the total upward flux, i.e. the sum of the diffusion flux and the dispersive flux, has to balance with the settling flux. Therefore, the opposite dispersive flux weakens the effect of the settling flux on the total vertical SSC profile. In addition, the SSC decreases in the region near the river bed and increases in the region near the water surface with the increase of the absolute value of the dispersive coefficient. However, when the absolute value of the dispersive coefficient is very large, the deviation between the predicted and measured SSC becomes larger again, while the sediment concentration changes from over-predicted to under-predicted within the half height of the flow depth.

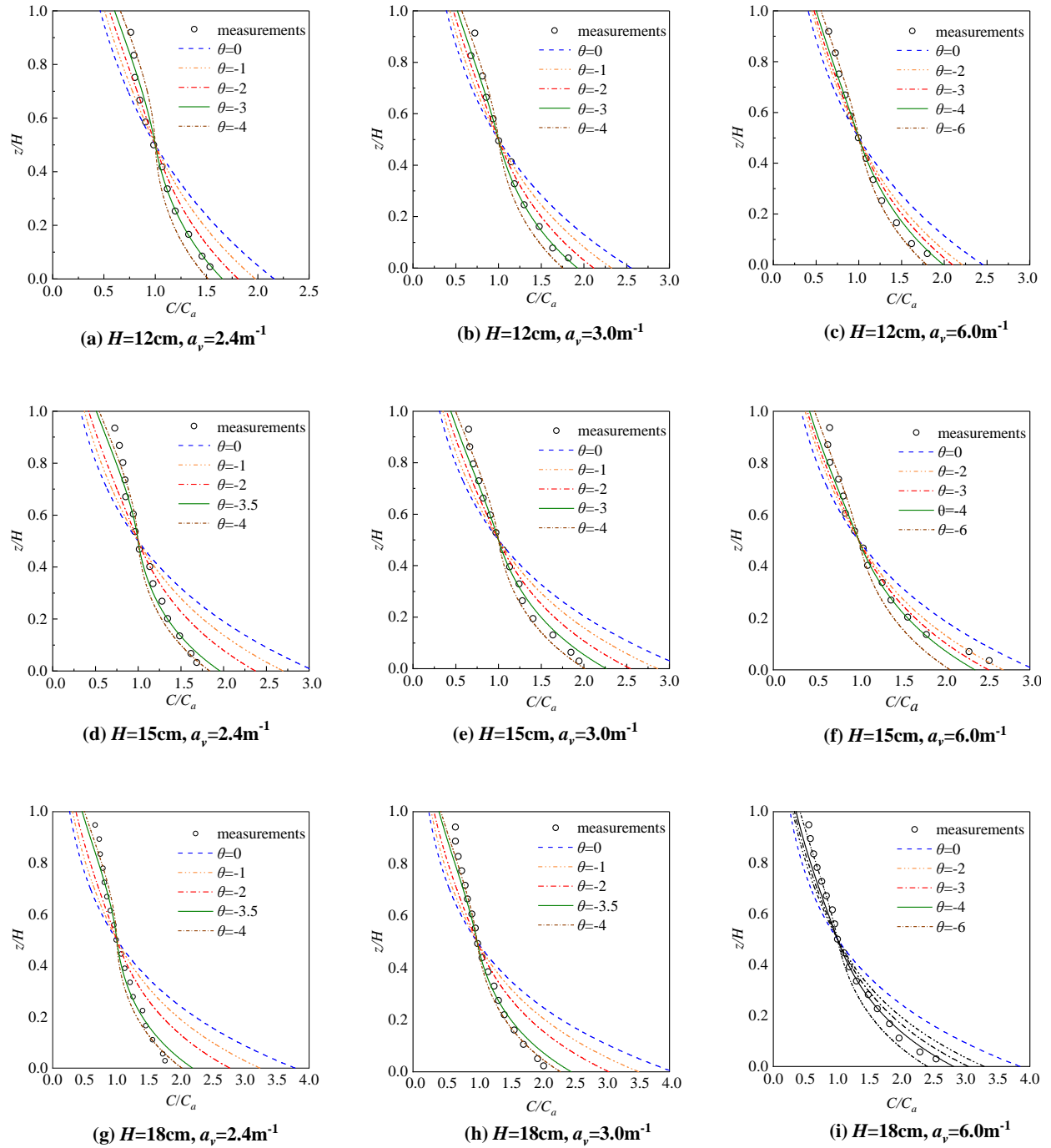
In Figure 5, values of H and a_v for different experiments are showed in the figure for convenience of comparison. Results with the same vegetation density but different flow depths (i.e. Figures 5(a), (d) and (g); Figures 5(b), (e) and (h); and Figures 5(c), (f) and (i)) show that the

437 relationship between the dispersive coefficient and flow depth is not very clear. However, the
 438 comparison of the same flow depth but different vegetation densities, i.e. Figures 5(a-c), (d-f)
 439 and (g-i), shows that the vegetation density has significant impact on the dispersive coefficient.
 440 Specifically, the maximum absolute values of the averaged fitting morphological coefficient are -
 441 10, -3.7, -3.5 and -4, corresponding respectively to the vegetation density of 1, 2.4, 3 and 6m^{-1} . In
 442 general, Figure 5 demonstrates that the absolute value of the morphological coefficient decreases
 443 with the increase of the vegetation density with the exception of the case $a_v = 6\text{m}^{-1}$. This
 444 exception case may be ascribed to the following fact: in the experiment of Lu (2008), the
 445 arrangement of the vegetation was regular and in the cases of D12/D15/D18-3, i.e. $a_v = 6\text{m}^{-1}$; the
 446 transverse and longitudinal interval between the vegetation centers was respectively 2cm and
 447 5cm. For this exception case, i.e. $a_v = 6\text{m}^{-1}$, the ratio of the transverse interval over the
 448 longitudinal interval was 0.4, while this ratio was approximate to one in the cases of $a_v = 1, 2.4$
 449 and 3m^{-1} . However, the conclusions of the dispersive rules and empirical coefficient α of
 450 Equation (15) are obtained from the experiments of stagger arrangement where the ratio of the
 451 transverse interval over the longitudinal interval is approximate to one. From this aspect, the
 452 unusual result for condition $a_v = 6\text{m}^{-1}$ may be caused by the arrangement of vegetation, which
 453 requires further experimental study for confirmation.



454
 455 **Figure 4.** Comparison of the vertical SSC profiles of the predicted (lines for different
 456 morphological conditions) by Equations (16a, b) and measured (open circles, Ikeda et al., 1991).

457



458

459 **Figure 5.** Comparison of the vertical SSC profiles of the predicted (lines for different
 460 morphological conditions) by Equations (16a, b) and experimentally measured (open circles, Lu,
 461 2008) for different vegetation heights and densities. As shown in figure: (a) D12-1; (b) D12-2;
 462 (c) D12-3; (d) D15-1; (e) D15-2; (f) D15-3; (g) D18-1; (h) D18-2; (i) D18-3.

463

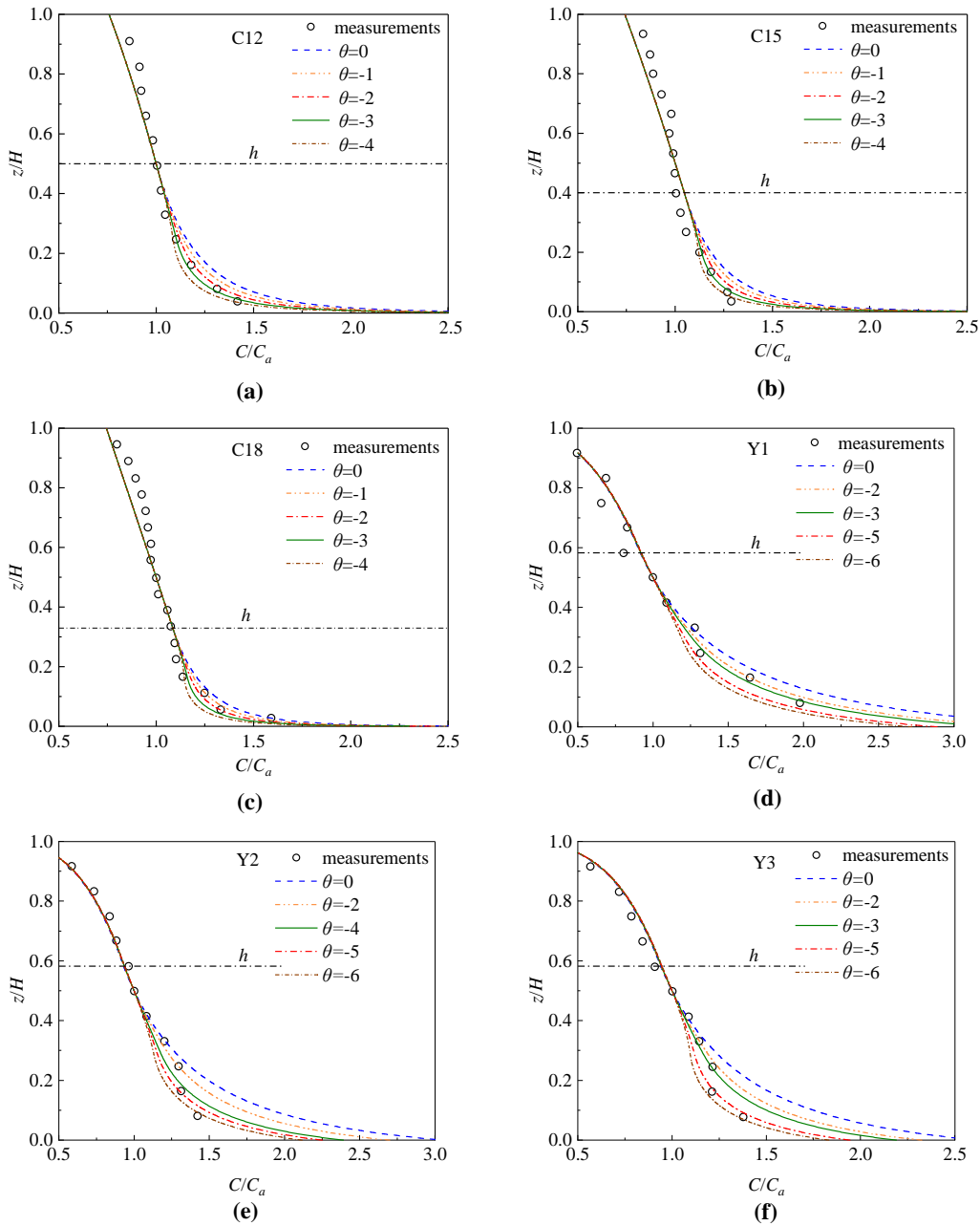
464 4.2 Submerged Vegetation

465 Figure 6 shows the comparison of the predicted and measured vertical SSC profiles in the
466 submerged vegetated open channel flows. In the experiments of Lu (2008), the ratio of the flow
467 depth over the vegetation height varies while the vegetation density is fixed (see Table 2 for
468 details of the flow conditions). Figures 6(a)(b)(c) show that the deviation of the predicted SSC
469 from the measured SSC decreases with the increase of the vegetation submergence for the
470 condition without the dispersive term (i.e. blue dashed lines). This indicates that the effect of the
471 vegetation on the vertical SSC profile is weakened with the increase of the vegetation
472 submergence (i.e. H/h increases). This may be because the relative importance of the vegetation
473 drag over the bed friction drag decreases for high vegetation submergence (Raupach et al., 1996;
474 Nepf & Vivoni, 2000; Nepf, 2012). Figures 6(a)(b)(c) show that $\theta=-3$ (i.e. green solid lines)
475 better represents the vegetation induced dispersive coefficient, indicating that the dispersive
476 coefficient has little relationship with the vegetation submergence for the flow conditions of Lu
477 (2008).

478 The values of the dispersive coefficient for the experiments of Yuuki and Okabe (2002)
479 are slightly larger than the values in the experiments of Lu (2008). This may be ascribed to the
480 fact that the vegetation structure in the experiments of Yuuki and Okabe (2002) favors the
481 dispersion. It is seen from Figure 6(d) that the vertical SSC profile can be reasonably predicted
482 with the dispersive coefficient $\theta=-3$, while Figures 6(e)(f) show that some deviations exist
483 between the predicted and the measured SSC. This may be due to the complicated vegetation
484 structure in their experiments, indicating that the analytical model proposed in this study has
485 some defects and cannot provide accurate prediction of the SSC in such complicated vegetation
486 structure. Nevertheless, the predicted SSC for the experiments of Yuuki and Okabe (2002) is
487 much better than the previous similar study (see Figure 10 in Yang and Choi (2010)), which did
488 not consider the effect of the dispersive term.

489 Analysis of the results shows that the analytical solution agrees well with experimental
490 measurements in the region of overflow. For regular arrangement of straight cylinders (i.e. the
491 experiments of Lu (2008)), $a_v=3\text{m}^{-1}$, the vertical SSC profile within the vegetation region can be
492 accurately predicted using the analytical approach proposed in this study with an appropriate
493 dispersive coefficient. For the staggered vegetation with complicated structure (i.e. the
494 experiments of Yuuki and Okabe (2002)), $a_v=2.08\text{m}^{-1}$, some deviation between the analytical
495 prediction and the measurement exists within the vegetation region. The variation of the vertical
496 SSC profile with the dispersive coefficient found in the emergent vegetated flow also appears in
497 the submerged vegetated flow, i.e. the SSC decreases with the increase of the absolute value of
498 the dispersive coefficient in the vegetated region.

499



500

501 **Figure 6.** The comparison between analytically predicted (lines) and experimentally measured
 502 (Lu (2008) and Yuuki and Okabe (2002): open circles) vertical SSC profile in the submerged
 503 vegetated flow.

504

505 4.3 Analysis

506 Result of Figures 4, 5 and 6 shows that the analytical solutions either over-predict or
 507 under-predict the SSC at different regions of the vegetated open channel sediment-laden flow. In

508 order to represent the deviation of the predicted SSC from the observed SSC for different values
 509 of θ , the averaged error (AE) is defined as following:

$$510 \quad AE = \frac{\sum (C_{pre} - C_{obs})}{N} \quad (26)$$

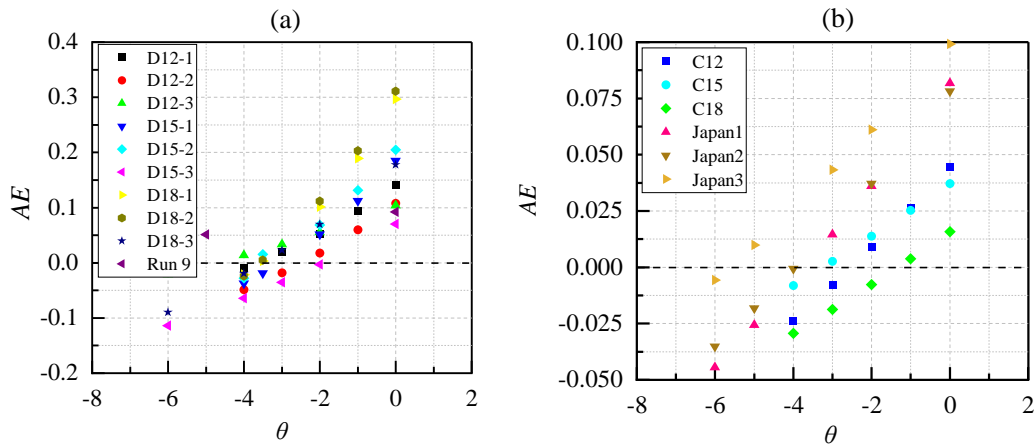
511 where N is the sampling number of the observed SSC in the vertical direction at a monitoring
 512 position in the experiments, C_{obs} is the observed SSC and C_{pre} represents the predicted SSC by
 513 the proposed model.

514 In order to determine the best-fitted value of θ , another common statistical parameter, i.e.
 515 the mean relative error (MRE), is also used to evaluate the error of the proposed model:

$$516 \quad MRE = \frac{\sum \frac{|C_{pre} - C_{obs}|}{C_{obs}}}{N} \quad (27)$$

517 Figure 7 shows the relationship between the AE and θ for both the emergent and the
 518 submerged vegetated open channel flow, which clearly demonstrates whether the model over-
 519 predicts or under-predicts SSC. It is seen from Figure 7 that the SSC is usually over-predicted by
 520 the proposed model (the positive value of AE) for the $\theta=0$. With the increase of the absolute
 521 value of θ , the SSC simulated by the proposed model varies from the over-predicted to the
 522 under-predicted (the negative value of AE) for both the submerged and the emergent vegetated
 523 open channel flow. The scope of θ corresponding to $AE=0$ in the emergent vegetated open
 524 channel flow is much more centralized than that in the channel with the submerged vegetation.
 525 The specific best-fitted value of θ can be determined by the variation of MRE calculated by
 526 Equation (27).

527

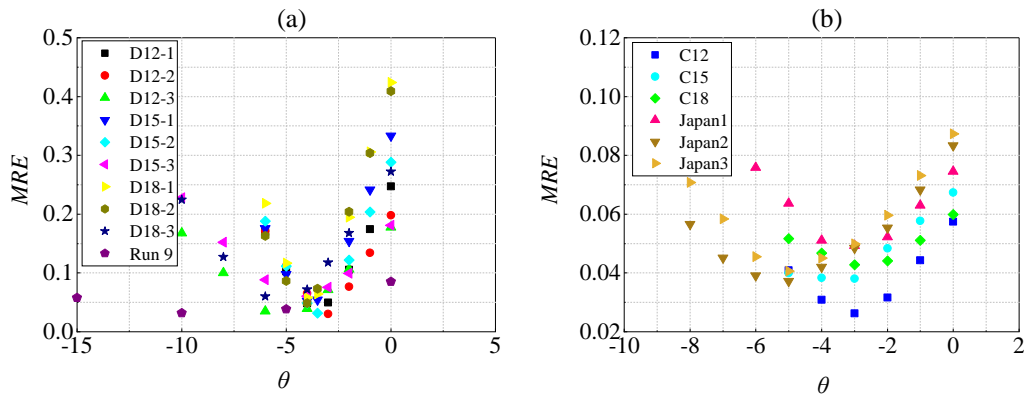


528

529 **Figure 7.** The variation of the vertical averaged error between the predicted and observed SSC
 530 with θ . (a) the emergent vegetated open channel flow; (b) the submerged vegetated open channel
 531 flow.

532

533 Figure 8 is the variation of MRE with θ for open channel flow with both the emergent
 534 (Figure 8(a)) and the submerged (Figure 8(b)) vegetation, respectively. Figure 8 shows that MRE
 535 decreases firstly and then increases with the increase of θ . The value of θ corresponding to the
 536 smallest MRE is known as the best-fitted value for that condition, which is listed in the last
 537 column of Table 3. Small MRE indicates that the model proposed in this study can accurately
 538 simulate the vertical profile of SSC in the vegetated open channel flow. The suggested value of
 539 θ is from -5 to -3 for the channels with the range of vegetation density a_v being from 2 to 6m^{-1} .
 540 More specifically, the best-fitted value of θ approximates to -4 with the range of the vegetation
 541 density being from 2 to 6m^{-1} in the open channel flow with the emergent vegetation. More
 542 experiments and studies are required to explore the rules of the dispersive coefficient in the open
 543 channel flow with the vegetation density outside the scope of $2\text{m}^{-1} < a_v < 6\text{m}^{-1}$.



544

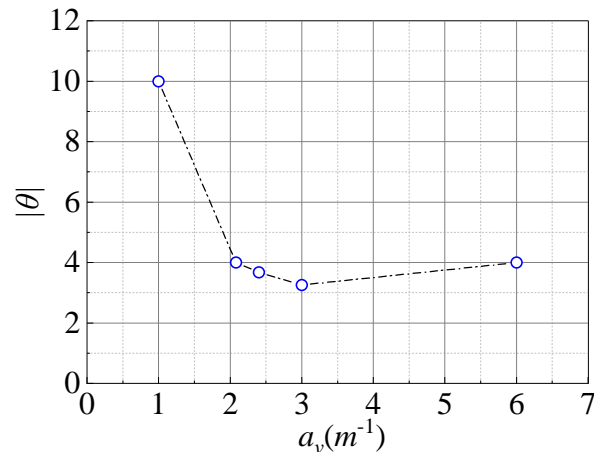
545 **Figure 8.** The variation of the MRE with θ : (a) the emergent vegetated open channel flow; (b)
 546 the submerged vegetated open channel flow.

547 **Table 3.** The parameters and the best-fitted value of θ for open channel flow with the emergent
 548 and the submerged vegetation.

Conditions	Run number	Re_s	$a_v(\text{m}^{-1})$	θ
Emergent vegetation	D12-1	1994	2.4	-3
	D12-2	1740	3	-3
	D12-3	1008	6	-4
	D15-1	1981	2.4	-4
	D15-2	1749	3	-3.5
	D15-3	1014	6	-4
	D18-1	2049	2.4	-4
	D18-2	1758	3	-4
	D18-3	1009	6	-4
Run 9	1420	1	-10	
Submerged vegetation	C12	991	3	-3
	C15	859	3	-3
	C18	753	3	-3
	Y1	153	2.08	-3
	Y2	187	2.08	-4
	Y3	217	2.08	-5

549 Above discussion shows that the magnitude of the dispersive coefficient is mainly
 550 influenced by the flow field (mainly velocity) and the vegetation characteristics (density,
 551 structure). The flow field can be represented by using the stem Reynolds number, i.e. $Re_s = \frac{u_w D}{\nu}$
 552 .The complicated vegetation structure enhances the dispersive strength through influencing the
 553 flow turbulence and the spatial heterogeneity, which can be proved by comparing the values of θ
 554 between the experiments of Yuuki and Okabe (2002) and the experiments of Lu (2008). Table 3
 555 lists the stem Reynolds number, the vegetation density and the best-fitted θ . The vegetation
 556 density for the experiments of Yuuki and Okabe (2002) (i.e. conditions Y1, Y2 and Y3) is all
 557 2.08, while the stem Reynolds number increases gradually. Therefore, the results of Y1, Y2 and
 558 Y3 indicate that the dispersion increases with the increase of Re_s , which may be caused by the
 559 strong turbulence induced by the large stem Reynolds number and corresponding intensive
 560 spatial heterogeneity. The value of θ for the experiments C12, C15 and C18 is all -3, while the
 561 stem Reynolds number varies slightly. This phenomenon may be ascribed to the fact that the
 562 vegetation structure of C12, C15 and C18 is regular and variation of the stem Reynolds number
 563 is small.

564 For both the emergent and the submerged vegetated open channel flow investigated in
 565 this study, Figure 9 shows that the averaged absolute value of θ decreases with the increase of
 566 the vegetation density, where θ is obtained by averaging the value of θ for the conditions of the
 567 same vegetation density. The results show that the gradient of the morphological coefficient with
 568 the vegetation density is large for the condition $a_v < 2.08 \text{m}^{-1}$, while the gradient is small for dense
 569 vegetation conditions investigated in this study. Within the vegetation region, the stem wakes
 570 become a localized source of turbulence such that the turbulent flow field is much more
 571 heterogeneous than that in the region without vegetation (Nepf et al., 1997). Thus, the dispersive
 572 coefficient is significantly increased by the presence of vegetation for small vegetation density.
 573 The interval between the vegetation stem's centers decreases gradually with the increase of the
 574 vegetation density, leading to the decrease of characteristic area of spatial averaging. Therefore,
 575 the vegetation-induced vortices may overlap in the characteristic area, which weakens the local
 576 inhomogeneity, and thus the dispersive coefficient decreases. Figure 9 also shows that the
 577 dispersive coefficient increases again when the vegetation density increases to $a_v = 6 \text{m}^{-1}$. This
 578 could be caused by the arrangement of vegetation for the case of $a_v = 6 \text{m}^{-1}$. More experiments are
 579 needed for better understanding and interpretation of the phenomenon.



580

581 **Figure 9.** The variation of the absolute value of the maximum morphological (dispersive)
582 coefficients with the vegetation density.

583

584 **5 Discussion**

585 The simulation of SSC in the vegetated open channel sediment-laden flow is very
586 complicated. It requires well-defined flow field including flow velocity and turbulence strength,
587 as well as the sediment particle characteristics. The empirical equations of the vertical turbulent
588 diffusion coefficient used for conditions of Lu (2008) are obtained from the previous flume
589 experiments (Nepf, 1999, 2004, 2012), which are interpreted as that the same straight rigid rods
590 are used as the experimental vegetation and the vegetation density is within the scope of these
591 formulas. For other conditions used in this study, experimental conditions are outside the scope
592 of these formulas. As such, the turbulent diffusion coefficient has to be determined by the
593 corresponding experimental observations or previous studies (Yang & Choi, 2010). The model
594 proposed in this study is based on the correct determination of the turbulent diffusion coefficient
595 model. Therefore, it is still a challenge task to extend the present model to open channel flow
596 with the natural live (flexible) vegetation. Nevertheless, the proposed model is a simple and
597 effective tool for simulating the vertical profile of SSC in the open channel flow with
598 vegetations.

599 The double-averaging method, in which the classical time-averaging advection-
600 diffusion equations are averaged over spatial area in the plane parallel to the bottom of channel,
601 is used to simulate the vertical SSC profile in the vegetated open channel flow. The application
602 of the double-averaging method for flow field analysis reduces the discordance resulted from the
603 spatial heterogeneity within the vegetation region. In order to solve the double-averaging
604 advection-diffusion equations, the diffusive flux is expressed by the Fickian diffusion model,
605 while the dispersive flux is the product of the dispersive coefficient K_D and the mass flux CU .
606 According to the previous experiments and the results of this study, the proposed dispersive
607 model generalizes the influences of the dispersion as the function of coordinate z . As such, the
608 size of the spatial averaging is not emphasized in this study. The suggestion about the size of the
609 spatial averaging is that it must represent the spatial heterogeneity to reduce the error induced by
610 the variation of the spatial averaging size. For example, it is correct to use the whole domain
611 parallel to the bed as the size of the spatial averaging for open channel flow with irregular
612 staggered vegetation or rough bed (Nikora et al., 2007b). For open channel flow with regular
613 staggered vegetation, the region of the adjacent four vegetations is suggested as the size of the
614 spatial averaging (Yuuki & Okabe, 2002; Poggi et al., 2004b).

615 There is little knowledge about the dispersive coefficient model, while most previous
616 investigations focused on the dispersive stress obtained from the experimental measurements.
617 Experiments with natural vegetation (*salix pentandra*) showed that the distribution of the
618 dispersive stress is very complicated (Righetti, 2008) in which the magnitude of the dispersive
619 stress at the top of vegetation and river bed is smaller than that at the half height of vegetation.
620 Poggi and Katul (2008b) and Coceal et al. (2008) carried out experiments using rigid straight
621 vegetation. Their results showed that the maximum value of the dispersive stress occurred at
622 almost the half height of vegetation and decreased toward both up and down vertical directions.
623 The results also showed that the magnitude of the dispersive stress greatly depended on the
624 vegetation density. Based on these laboratory experimental studies, the authors assume that the

625 variation of the dispersive flux, i.e. $\langle u_3 "c" \rangle = -K_D UC$, in the vegetated open channel flow is
 626 similar to that of the dispersive stress. For simplification, the authors further assume that the
 627 dispersive coefficient K_D is a triangle profile in the vegetation region as expressed in Equations
 628 (12) and (13). The comparison of the SSC profile simulated by proposed model with the
 629 experimental measurements confirms the strong relation between dispersive coefficient and the
 630 vertical SSC profile in the vegetated open channel flows.

631 Results show that the dispersive term (usually appearing as negative value) plays an
 632 important role in determining the vertical SSC profile in the vegetated suspended sediment-laden
 633 flow. For the emergent vegetated flow, the model calculated SSC from the half height of the
 634 vegetation to the channel bottom varies from over-prediction to under-prediction with the
 635 increase of the absolute value of the dispersive coefficient, while the predicted SSC above the
 636 half height of vegetation has opposite variation trend (see Figures 4 and 5). For the submerged
 637 vegetated flow, the variation of SSC within the vegetation region is similar to that under the half
 638 height of vegetation of the emergent vegetated flow (see Figure 6). This means that the
 639 appropriate dispersive coefficient can be obtained by fitting the experimental data. Because all
 640 the dispersive coefficients are modeled as triangle profile, the maximum value of the
 641 morphologic coefficient (i.e. θ) is used to represent the magnitude of the dispersive coefficient.
 642 The relationship between the best-fitted value of θ and the vegetation density, the vegetation
 643 structure and the stem Reynolds number depends on the experimental conditions. This means
 644 that the best-fitted values of θ proposed in this paper can only represent the conditions
 645 investigated in this study. However, the rules between θ and a_v , Re_s and the vegetation structure
 646 conform to the physical mechanism and are strongly supported by previous relevant
 647 experimental studies.

648

649 **6 Conclusions**

650 In this paper, the model of the dispersive coefficient is proposed based on the concept of
 651 the dispersion to investigate the vertical SSC profile in the vegetated suspended sediment-laden
 652 flow. The double-averaging method is applied to simulate the vertical SSC profile in the
 653 vegetated open channel flow with time-spatial averaging advection-diffusion equations. The
 654 proposed model is validated by comparing the analytical solution of the vertical SSC profile with
 655 the existing experimental measurements. Results show that the proposed model of the dispersive
 656 coefficient is reliable and can be used to estimate the vertical SSC profile in the complicated
 657 vegetated, sediment-laden open channel flow. The following conclusions can be drawn from this
 658 study.

659 (1) A model for estimating the dispersive coefficient is proposed in this study based on
 660 the concept of the dispersion. For both the emergent and the submerged vegetated open channel
 661 flow investigated in this study, the dispersive coefficient decreases with the increase of the
 662 vertical axis z from the half height of the vegetation and increases with the increase of z from the
 663 channel bottom to the half height of vegetation. The dispersive coefficient reaches zero at both
 664 the top of the vegetation and the channel bottom.

665 (2) The effect of the dispersion on the vertical SSC profile within the vegetation region is
 666 significant and cannot be ignored. The inclusion of the dispersive term can greatly improve the
 667 prediction of the vertical SSC profile in the vegetated region and the region close to the channel

668 bottom. The dispersive term can be extended to the roughness bed or rivers with sand ripples,
 669 where the spatial heterogeneity of flow structure is also strong owing to the complicated uneven
 670 channel morphology.

671 (3) The double-averaging method is applied to simulate the vertical SSC profile in the
 672 vegetated open channel flow for improving the prediction of SSC. This is particularly important
 673 in the region of vegetation, where the spatial heterogeneity of the turbulent flow is strong owing
 674 to the presence of vegetation.

675 (4) The fitted morphological coefficient is mainly related to the vegetation density, the
 676 flow field and the vegetation structure in this study. For the conditions investigated in this study,
 677 the absolute values of the morphological and the dispersive coefficients decrease sharply with
 678 the increase of vegetation density, then increase slightly with the increase of vegetation density.

679 (5) The suggested range of θ is -5 to -3 with the mean related error smaller than 10%
 680 when the vegetation density a_v is within the range from 2 to 6m^{-1} . Owing to the limited available
 681 experimental data, it is not clear what is the variation trend of the dispersive coefficient for
 682 sparse vegetation density (i.e. $a_v < 1\text{m}^{-1}$) and very dense vegetation density (i.e. $a_v > 6\text{m}^{-1}$). Further
 683 experiments with a wide range of the vegetation density are required to accurately propose the
 684 dispersive model.

685

686 **Acknowledgments**

687 All the data used in this work have been reported elsewhere (Ikeda et al., 1991; Yuuki & Okabe,
 688 2002; Lu, 2008). The research reported here is financially supported by the Natural Science
 689 Foundation of China (Nos. 11872285 and 11672213), The UK Royal Society – International
 690 Exchanges Program (IES\R2\181122) and the Open Funding of State Key Laboratory of Water
 691 Resources and Hydropower Engineering Science (WRHES), Wuhan University (Project No:
 692 2018HLG01). Comments made by Reviewers have greatly improved the quality of the final
 693 paper.

694 There are no real or perceived financial conflicts of interests for any author, no other affiliations
 695 for any author that may be perceived as having a conflict of interest with respect to the results of
 696 this paper.

697

698 **Nomenclature**

A	integral constant
a_v	the frontal area density of vegetation
b_1, b_2	parameters of expression of turbulent diffusion coefficient profile at region $z < h$ and $z \geq h$ respectively in submerged vegetated open channel flows
C	time-spatial averaging suspended sediment concentration
C_a	referenced suspended sediment concentration at referenced height
C_D	drag coefficient of vegetation

C_{pre}	predicted suspended sediment concentration by this model
C_{obs}	observed suspended sediment concentration in experiments
c	instantaneous suspended sediment concentration
D	diameter of vegetation
d	representative size of sediment particles
f, φ	two different variables
g	acceleration of gravity
H	flow depth
h	height of vegetation
K_D	dispersive coefficient
K_f	a scale factor and $K_f=0.001$ in present study
K_m	molecular diffusion coefficient
K_z	vertical turbulent diffusion coefficient
k	von Karman's constant
k_1, k_2	gradients of expression of turbulent diffusion coefficient profile at region $z < h$ and $z \geq h$ respectively in submerged vegetated open channel flows
k_m	morphological coefficient
N	sampled number of the observed SSC in the vertical direction at a monitor point in the experiments
n	number of vegetation per unit area
r_1, λ_1	two parameters
Re_s	stem Reynolds number
r_2, λ_2	two parameters
S	source or sink of sediment in advection-diffusion equation
s	slope of channel bed
t	time
U	averaged longitudinal flow velocity of cross-section
u	instantaneous longitudinal flow velocity
u_*	friction velocity
u_w	averaged velocity in the wake region of vegetation
u_H	flow velocity at the water surface
u_j	instantaneous flow velocity component in j th direction

u_1, u_2, u_3	instantaneous flow velocity of longitudinal, transverse and vertical, respectively
x_j	the j th direction, $x_1=x$, $x_2=y$ and $x_3=z$ are directions of longitudinal, transverse and vertical, respectively
z	vertical coordinate
z_a	referenced height
α	a proportional factor
γ_f	the bulk density of water
γ_s	the bulk density of sediment
σ	a constant
ν	the kinematic viscosity of water
ω	settling velocity of sediment particles
θ	values of morphological coefficient at the half height of vegetation
Δu	velocity difference between the region of vegetation wake and overflow
'	the deviation of instantaneous variables from time averaging variables
"	the deviations of time averaged variables from spatial averaged variables
-	time average
< >	spatial average
< - >	time-spatial average

699

700 **References**

- 701 Boudreault, L., Dupont, S., Bechmann, A., & Dellwik, E. (2017). How forest inhomogeneities
702 affect the edge flow. *Boundary-Layer Meteorology*, 162(3), 375-400.
703 <https://doi.org/10.1007/s10546-016-0202-5>
- 704 Coceal, O., Thomas, T. G., & Belcher, S. E. (2007). Spatial Variability of Flow Statistics within
705 Regular Building Arrays. *Boundary-Layer Meteorology*, 125(3), 537-552.
706 <https://doi.org/10.1007/s10546-007-9206-5>
- 707 Coceal, O., Thomas, T. G., & Belcher, S. E. (2008). Spatially-averaged flow statistics within a
708 canopy of large bluff bodies: Results from direct numerical simulations. *Acta*
709 *Geophysica*, 56(3), 862-875. <https://doi.org/10.2478/s11600-008-0025-y>
- 710 Coceal, O., Thomas, T. G., Castro, I. P., & Belcher, S. E. (2006). Mean Flow and Turbulence
711 Statistics over Groups of Urban-like Cubical Obstacles. *Boundary-Layer Meteorology*,
712 121(3), 491-519. <https://doi.org/10.1007/s10546-006-9076-2>
- 713 Elder, J. W. (1959). The dispersion of marked fluid in turbulent shear flow, *Journal of Fluid*
714 *Mechanics*, 5(4), 544-560. <https://doi.org/10.1017/S0022112059000374>

- 715 Florens, E., Eiff, O., & Moulin, F. (2013). Defining the roughness sublayer and its turbulence
716 statistics. *Experiments in Fluids*, 54(4). <https://doi.org/10.1007/s00348-013-1500-z>
- 717 Fu, X. D., Wang, G. Q., & Shao, X. (2005). Vertical dispersion of fine and coarse sediments in
718 turbulent open-channel flows, *Journal of Hydraulic Engineering*, 10(131), 877-888.
719 [https://doi.org/10.1061/\(ASCE\)0733-9429\(2005\)131:10\(877\)](https://doi.org/10.1061/(ASCE)0733-9429(2005)131:10(877))
- 720 Han, X., He, G. J., & Fang, H. W. (2017). Double-averaging analysis of turbulent kinetic energy
721 fluxes and budget based on large-eddy simulation. *Journal of Hydrodynamics*, 29(4),
722 567-574. [https://doi.org/10.1016/S1001-6058\(16\)60769-2](https://doi.org/10.1016/S1001-6058(16)60769-2)
- 723 Huai, W. X., Chen, Z. B., Han, J., Zhang, L. X., & Zeng, Y. H. (2009b). Mathematical model for
724 the flow with submerged and emerged rigid vegetation. *Journal of Hydrodynamics*,
725 21(5), 722-729. [https://doi.org/10.1016/S1001-6058\(08\)60205-X](https://doi.org/10.1016/S1001-6058(08)60205-X)
- 726 Huai, W. X., Yang, L., Wang, W. J., Guo, Y. K., Wang, T., & Cheng, Y. G. (2019). Predicting
727 the vertical low suspended sediment concentration in vegetated flow using a random
728 displacement model. *Journal of Hydrology*, 578, 124101.
729 <https://doi.org/10.1016/j.jhydrol.2019.124101>
- 730 Huai, W. X., Zeng, Y. H., Xu, Z. G., & Yang, Z. H. (2009a). Three-layer model for vertical
731 velocity distribution in open channel flow with submerged rigid vegetation. *Advances in*
732 *Water Resources*, 32(4), 487-492. <https://doi.org/10.1016/j.advwatres.2008.11.014>
- 733 Ikeda, S., Izumi, N., & Ito, R. (1991). Effects of pile dikes on flow retardation and sediment
734 transport. *Journal of Hydraulic Engineering*, 11(117), 1459-1478.
735 [https://doi.org/10.1061/\(ASCE\)0733-9429\(1991\)117:11\(1459\)](https://doi.org/10.1061/(ASCE)0733-9429(1991)117:11(1459))
- 736 Kim, H. S., Kimura, I., & Park, M. (2018). Numerical simulation of flow and suspended
737 sediment deposition within and around a circular patch of vegetation on a rigid bed.
738 *Water Resources Research*, 54(10), 7231-7251. <https://doi.org/10.1029/2017WR021087>
- 739 Kundu, S. (2019). Modeling stratified suspension concentration distribution in turbulent flow
740 using fractional advection–diffusion equation, *Environmental Fluid Mechanics*, 19(6),
741 1557-1574. <https://doi.org/10.1007/s10652-019-09679-9>
- 742 Le Bouteiller, C., & Venditti, J. G. (2015). Sediment transport and shear stress partitioning in a
743 vegetated flow, *Water Resources Research*, 51(4), 2901-2922.
744 <https://doi.org/10.1002/2014WR015825>
- 745 Li, D., Yang, Z. H., Sun, Z., Huai, W. X., & Liu, J. (2018). Theoretical model of suspended
746 sediment concentration in a flow with submerged vegetation. *Water*, 10(11), 1656.
747 <https://doi.org/10.3390/w10111656>
- 748 Li, S., & Katul, G. (2019). Cospectral budget model describes incipient sediment motion in
749 turbulent flows. *Physical Review Fluids*, 4(9), 093801.
750 <https://doi.org/10.1103/PhysRevFluids.4.093801>
- 751 Li, S., Katul, G., & Huai, W. (2019). Mean velocity and shear stress distribution in floating
752 treatment wetlands: An analytical study. *Water Resources Research*, 55(8), 6436-6449.
753 <https://doi.org/10.1029/2019WR025131>
- 754 Li, S., Shi, H., Xiong, Z., Huai, W., & Cheng, N. (2015). New formulation for the effective
755 relative roughness height of open channel flows with submerged vegetation. *Advances in*
756 *Water Resources*, 86, 46-57. <https://doi.org/10.1016/j.advwatres.2015.09.018>

- 757 Lu, S. Q. (2008). Experimental study on suspended sediment distribution in flow with rigid
758 vegetation, (Doctoral dissertation). Hohai University, Nanjing, Jiangsu, China (in
759 Chinese).
- 760 Moltchanov, S., Bohbot, R. Y., Duman, T., & Shavit, U. (2015). Canopy edge flow: A
761 momentum balance analysis. *Water Resources Research*, 51(4), 2081-2095.
762 <https://doi.org/10.1002/2014WR015397>
- 763 Nepf, H. M. (1999). Drag, turbulence, and diffusion in flow through emergent vegetation. *Water*
764 *Resources Research*, 2(35), 479-489. <https://doi.org/10.1029/1998WR900069>
- 765 Nepf, H. M. (2004). Vegetated flow dynamics. In S. Fagherazzi, M. Marani, L. K. Blum (Eds.),
766 *The Ecogeomorphology of Tidal Marshes* (Vol. 59, pp. 137-163). Washington, DC:
767 American Geophysical Union. <https://doi.org/10.1029/CE059p0137>
- 768 Nepf, H. M. (2012). Flow and transport in regions with aquatic vegetation. *Annual Review of*
769 *Fluid Mechanics*, 44(1), 123-142. <https://doi.org/10.1146/annurev-fluid-120710-101048>
- 770 Nepf, H. M., Sullivan, J. A., & Zavistoski, R. A. (1997). A model for diffusion within emergent
771 vegetation. *Limnology and Oceanography*, 42(8), 1735-1745.
772 <https://doi.org/10.4319/lo.1997.42.8.1735>
- 773 Nepf, H. M., & Vivoni, E. R. (2000). Flow structure in depth-limited, vegetated flow. *Journal of*
774 *Geophysical Research: Oceans*, 105(C12), 28547-28557.
775 <https://doi.org/10.1029/2000jc900145>
- 776 Nikora, V., McEwan, I., McLean, S., Coleman, S., Pokrajac, D., & Walters, R. (2007a). Double-
777 averaging concept for rough-bed open-channel and overland flows: theoretical
778 background. *Journal of Hydraulic Engineering*, 133(8), 873-883.
779 [https://doi.org/10.1061/\(ASCE\)0733-9429\(2007\)133:8\(873\)](https://doi.org/10.1061/(ASCE)0733-9429(2007)133:8(873))
- 780 Nikora, V., McLean, S., Coleman, S., Pokrajac, D., McEwan, I., & Campbell, L. (2007b).
781 Double-averaging concept for rough-bed open-channel and overland flows: applications.
782 *Journal of Hydraulic Engineering*, 133(8), 884-895.
783 [https://doi.org/10.1061/\(ASCE\)0733-9429\(2007\)133:8\(884\)](https://doi.org/10.1061/(ASCE)0733-9429(2007)133:8(884))
- 784 Poggi, D., & Katul, G. G. (2008a). Micro- and macro-dispersive fluxes in canopy flows. *Acta*
785 *Geophysica*, 56(3), 778-799. <https://doi.org/10.2478/s11600-008-0029-7>
- 786 Poggi, D., & Katul, G. G. (2008b). The effect of canopy roughness density on the constitutive
787 components of the dispersive stresses. *Experiments in Fluids*, 45(1), 111-121.
788 <https://doi.org/10.1007/s00348-008-0467-7>
- 789 Poggi, D., Katul, G. G., & Albertson, J. D. (2004b). A note on the contribution of dispersive
790 fluxes to momentum transfer within canopies. *Boundary-Layer Meteorology*, 111(3),
791 615-621. <https://doi.org/10.1023/b:boun.0000016563.76874.47>
- 792 Poggi, D., Porporato, A., & Ridolfi, L. (2004a). The effect of vegetation density on canopy sub-
793 layer turbulence. *Boundary-Layer Meteorology*, 111(3), 565-587.
794 <https://doi.org/10.1023/b:boun.0000016576.05621.73>
- 795 Raupach, M. R., Finnigan, J. J., & Brunei, Y. (1996). Coherent eddies and turbulence in
796 vegetation canopies: The mixing-layer analogy. *Boundary-Layer Meteorology*, 78(3-4),
797 351-382. <https://doi.org/10.1007/BF00120941>

- 798 Righetti, M. (2008). Flow analysis in a channel with flexible vegetation using double-averaging
799 method. *Acta Geophysica*, 56(3), 801-823. <https://doi.org/10.2478/s11600-008-0032-z>
- 800 Rouse, H. (1937). Modern conceptions of the mechanics of fluid turbulence. *Transactions of*
801 *American Society of Civil Engineers*, 102, 463–505.
- 802 Sonnenwald, F., Stovin, V., & Guymier, I. (2019). Estimating drag coefficient for arrays of rigid
803 cylinders representing emergent vegetation. *Journal of Hydraulic Research*, 57(4), 591-
804 597. <https://doi.org/10.1080/00221686.2018.1494050>
- 805 Spiller, S. M., Rütger, N., & Baumann, B. (2015). Form-induced stress in non-uniform steady
806 and unsteady open channel flow over a static rough bed. *International Journal of*
807 *Sediment Research*, 30(4), 297-305. <http://dx.doi.org/10.1016/j.ijsrc.2014.10.002>
- 808 Stoesser, T., & Nikora, V. I. (2008). Flow structure over square bars at intermediate
809 submergence: Large Eddy Simulation study of bar spacing effect. *Acta Geophysica*,
810 56(3), 876-893. <https://doi.org/10.2478/s11600-008-0030-1>
- 811 Tan, G. M., Fang, H. W., Dey, S., & Wu, W. M. (2018). Rui-jin zhang's research on sediment
812 transport. *Journal of Hydraulic Engineering*, 144(6), 02518002.1-02518002.6.
813 [https://doi.org/10.1061/\(ASCE\)HY.1943-7900.0001464](https://doi.org/10.1061/(ASCE)HY.1943-7900.0001464)
- 814 Tanino, Y., & Nepf, H. M. (2008a). Lateral dispersion in random cylinder arrays at high
815 Reynolds number. *Journal of Fluid Mechanics*, 600, 339-371.
816 <https://doi.org/10.1017/S0022112008000505>
- 817 Tanino, Y., & Nepf, H. M. (2008b). Laboratory investigation of mean drag in a random array of
818 rigid, emergent cylinders. *Journal of Hydraulic Engineering*, 134(1), 34-41.
819 [https://doi.org/10.1061/\(ASCE\)0733-9429\(2008\)134:1\(34\)](https://doi.org/10.1061/(ASCE)0733-9429(2008)134:1(34))
- 820 Termini, D. (2019). Turbulent mixing and dispersion mechanisms over flexible and dense
821 vegetation. *Acta Geophysica*, 67(3), 961-970. [https://doi.org/10.1007/s11600-019-00272-
822 8](https://doi.org/10.1007/s11600-019-00272-8)
- 823 Tsai, C. W., & Huang, S. H. (2019). Modeling suspended sediment transport under influence of
824 turbulence ejection and sweep events. *Water Resources Research*, 55(7), 5379-5393.
825 <https://doi.org/10.1029/2018WR023493>
- 826 van Rijn, L. C. (1984). Sediment transport, part II: suspended load transport. *Journal of*
827 *Hydraulic Engineering*, 110(11), 1613-1641.
828 [https://doi.org/10.1061/\(ASCE\)0733-9429\(1984\)110:11\(1613\)](https://doi.org/10.1061/(ASCE)0733-9429(1984)110:11(1613))
- 829 Västilä, K., & Järvelä, J. (2018). Characterizing natural riparian vegetation for modeling of flow
830 and suspended sediment transport. *Journal of Soils and Sediments*, 18(10), 3114-3130.
831 <https://doi.org/10.1007/s1136>
- 832 Wang, W., Huai, W. X., & Gao, M. (2014). Numerical investigation of flow through vegetated
833 multi-stage compound channel. *Journal of Hydrodynamics*, 26(3), 467-473.
834 [https://doi.org/10.1016/S1001-6058\(14\)60053-6](https://doi.org/10.1016/S1001-6058(14)60053-6)
- 835 Wang, X. Y., Xie, W. M., Zhang, D., & He, Q. (2016). Wave and vegetation effects on flow and
836 suspended sediment characteristics: A flume study. *Estuarine, Coastal and Shelf Science*,
837 182, 1-11. <http://dx.doi.org/10.1016/j.ecss.2016.09.009>

- 838 Wilson, C. A. M. E. (2007). Flow resistance models for flexible submerged vegetation. *Journal*
839 *of Hydrology*, 342(3-4), 213-222. <https://doi.org/10.1016/j.jhydrol.2007.04.022>
- 840 Yang, J. Q., & Nepf, H. M. (2019), Impact of Vegetation on Bed Load Transport Rate and
841 Bedform Characteristics, *Water Resources Research*, 55(7), 6109-6124.
842 <https://doi.org/10.1029/2018WR024404>
- 843 Yang, W., & Choi, S. (2010). A two-layer approach for depth-limited open-channel flows with
844 submerged vegetation. *Journal of Hydraulic Research*, 48(4), 466-475.
845 <https://doi.org/10.1080/00221686.2010.491649>
- 846 Yuuki, T., & Okabe, T. (2002). Hydrodynamic mechanism of suspended load on riverbeds
847 vegetated by woody plants. *Proceedings of Hydraulic Engineering*, 46, 701–706 (in
848 Japanese). <https://doi.org/10.2208/prohe.46.701>
- 849 Zhang, R. J., & Xie, J. H. (1989). River sediment dynamics (in Chinese). Beijing, CHN: China
850 Water and Power Press. ISBN: 9787801244260.
- 851